Gatekeeper Tyrosine Phosphorylation of SYMRK Is Essential for Synchronizing the Epidermal and Cortical Responses in Root Nodule Symbiosis[1]

Sudip Saha, Anindita Paul, Laura Herring[2], Ayan Dutta, Avisek Bhattacharya, Sandip Samaddar[3], Michael B. Goshe, and Maitrayee DasGupta*

Department of Biochemistry, University of Calcutta, Kolkata 700019, India (S. Saha, A.P., A.D., A.B., S. Samaddar, M.D.); and Department of Molecular and Structural Biochemistry, North Carolina State University, Raleigh, North Carolina 27695 (L.H., M.B.G.)

ORCID IDs: 0000-0001-9742-3306 (S. Saha); 0000-0003-4496-7312 (L.H.); 0000-0002-7260-3746 (M.D.).

Symbiosis receptor kinase (SYMRK) is indispensable for activation of root nodule symbiosis (RNS) at both epidermal and cortical levels and is functionally conserved in legumes. Previously, we reported SYMRK to be phosphorylated on "gatekeeper" Tyr both in vitro as well as in planta. Since gatekeeper phosphorylation was not necessary for activity, the significance remained elusive. Herein, we show that substituting gatekeeper with nonphosphorylatable residues like Phe or Ala significantly affected autophosphorylation on selected targets on activation segment/αEF and β3-αC loop of SYMRK. In addition, the same gatekeeper mutants failed to restore proper symbiotic features in a *symrk* null mutant where rhizobial invasion of the epidermis and nodule organogenesis was unaffected but rhizobia remain restricted to the epidermis in infection threads migrating parallel to the longitudinal axis of the root, resulting in extensive infection patches at the nodule apex. Thus, gatekeeper phosphorylation is critical for synchronizing epidermal/cortical responses in RNS.

The establishment of root nodule symbiosis (RNS) involves rhizobial invasion in the root epidermis and nodule organogenesis in the root cortical cells. In the epidermis, recognition of compatible rhizobia induces root hair curls in the host plant to entrap the rhizobia in an infection pocket (Gage, 2004). In these infection pockets or chambers, rhizobia multiply to form a microcolony that is believed to generate threshold levels of bacterial signal molecules required for initiation and progression of infection threads (ITs) through the epidermis into the cortex of the root (Fournier et al., 2015). A compatible host-symbiont interaction in the epidermis also leads to formation of nodule primordia in the cortex, where eventually the rhizobia is endocytically accommodated from the invading ITs to develop nitrogen-fixing symbiosomes in mature nodules. The epidermal and cortical processes are coordinated both spatially and temporally to ensure rhizobial accommodation in the subtending nodule primordia (Popp and Ott, 2011; Oldroyd, 2013; Miri et al., 2016).

At the molecular level, these host responses are initiated with the recognition of rhizobial Nod factors by two LysM receptor-like kinases (RLKs): NFR1 and NFR5 in *Lotus japonicus* and lysin motif domain-containing RLK-3 (LYK3) and NFP in *Medicago truncatula* (Limpens et al., 2003; Madsen et al., 2003; Broghammer et al., 2012). Recently, another Nod factor-induced LysM-RLK (exopolysaccharide receptor 3) was shown to monitor rhizobial EPS structures in *Lotus*, indicating a two-stage mechanism involving sequential receptor-mediated recognition of Nod factor and EPS signals to ensure host symbiont compatibility (Kawaharada et al., 2015). Following the perception of Nod factors, Ca^{2+} influx at the tip of the root hair and Ca^{2+} spiking at the perinuclear region of the root hair are induced (Oldroyd, 2013). Components that function upstream of Ca^{2+} spiking include Symbiosis Receptor Kinase (SYMRK)/ Doesn't Make Infections (DMI) 2

[1] This work was financially supported by grants from the government of India: DBT-CEIB (Centre of Excellence and Innovation in Biotechnology), BT/01/CEIB/09/VI/10 (to M.D.), DBT-IPLS, BT/PR14552/INF/22/123/2010, and fellowships to S. Saha (CSIR 09/028(0830)/2010-EMR-I), A.P. (UGC/1269), A.D. (RFSMS/F.5-19/2007BSR), and A.B. (UGC/307). This work was also funded by a grant from the U.S. National Science Foundation (DBI-1126244 to M.B.G.).

[2] Present address: Proteomics Core, University of North Carolina, Chapel Hill, NC 27695.

[3] Present address: New Chemistry Unit, Jawaharlal Nehru Centre for Advanced Scientific Research, Bangalore 560064, India.

* Address correspondence to maitrayee_d@hotmail.com.

The author responsible for distribution of materials integral to the findings presented in this article in accordance with the policy described in the Instructions for Authors (www.plantphysiol.org) is: Maitrayee DasGupta (maitrayee_d@hotmail.com).

S. Saha, A.P., L.H., A.D., A.B., and S. Samaddar performed research; S. Saha conducted phenotypic techniques; A.P., A.B., and S. Samaddar conducted biochemical techniques; A.D. and A.B. conducted recombinant techniques; L.H. and M.B.G. conducted mass spectrometry; S. Saha, A.P., and M.D.G. designed, analyzed, and interpreted data and wrote the paper.

www.plantphysiol.org/cgi/doi/10.1104/pp.15.01962

(Endre et al., 2002; Stracke et al., 2002), the nuclear envelope-localized cation channels, and components of the nucleopore complex. A nuclear calcium- and calmodulin-dependent protein kinase (CCaMK/DMI3; Lévy et al., 2004; Mitra et al., 2004) decodes the Ca^{2+} spiking and phosphorylates a transcription factor (TF) CYCLOPS/Interacting Protein of DMI3 (IPD3; Messinese et al., 2007; Singh et al., 2014), which along with several other TFs orchestrates the gene expression required for rhizobial infection and nodule organogenesis (Oldroyd, 2013; Suzaki et al., 2015).

SYMRK is a functionally conserved central component of symbiotic signaling that experienced structural diversification during evolution (Markmann et al., 2008). It contains an ectodomain composed of a malectin-like domain and a Leu-rich repeat region. Unlike the *nfr* mutants that lack most cellular and physiological responses, including induction of Ca^{2+} influx and Ca^{2+}-spiking in response to rhizobia, the root hairs of *symrk* mutants respond with Ca^{2+} influx but not with Ca^{2+}-spiking and do not develop ITs, indicating SYMRK to be positioned downstream of the NFRs (Miwa et al., 2006). Recently, *Lj*SYMRK was shown to interact with NFR5 through its ectodomain, suggesting a role of SYMRK in initiating symbiotic signaling in concert with the NFRs (Antolín-Llovera et al., 2014a). Unlike the NFRs, specificity of recognition of bacterial partners in RNS is independent of the source of SYMRK (Gherbi et al., 2008; Markmann et al., 2008; Saha et al., 2014). SYMRK is indispensable at both epidermal and cortical levels and is important for coupling the epidermal/cortical events in RNS guided by a GDPC motif in its ectodomain (Kosuta et al., 2011; Antolín-Llovera et al., 2014a). The kinase activity of SYMRK is also vital for its role in symbiosis, as several SYMRK mutants have missense or nonsense mutations in the catalytic domain (Yoshida and Parniske, 2005). Several interactors are known for SYMRK that indicated this RLK to be nodal to various downstream cellular responses associated with inception of RNS (Antolín-Llovera et al., 2014b).

The majority of plant RLKs including SYMRK are distinguished by having Tyr in the "gatekeeper" position adjacent to the hinge region of their kinase domains (Shiu and Bleecker, 2001). This residue helps dictate the size of a hydrophobic pocket that forms in the DFG-out conformation of protein kinases (Hari et al., 2013; Sohl et al., 2015). Though the gatekeeper residue is important primarily because it is the architect of this deep catalytic cleft, several lines of evidence now indicate that protein kinases have adopted mechanisms of regulation mediated by their gatekeeper residues (Emrick et al., 2006; Chen et al., 2007; Azam et al., 2008). Most importantly, oncogenic activation of several receptor Tyr kinases (RTKs) has been shown to be due to changes in the gatekeeper (Azam et al., 2008). The importance of the gatekeeper Tyr residue is also emerging in the well-characterized RLKs like brassinosteroid-insensitive 1 (BRI1) and LYK3 or receptor-like cytoplasmic kinase like Botrytis-induced kinase 1 (BIK1), where structure-mimic substitutions of the gatekeeper affect either kinase activity or biological activity or both (Oh et al., 2009a, 2009b; Klaus-Heisen et al., 2011; Lin et al., 2014). RLKs are also shown to adopt an active conformation by forming a hydrogen-bonded triad between the invariant Lys-Glu salt-bridge and the gatekeeper Tyr (Bojar et al., 2014). But considering the contrasting effects of the gatekeeper substitution in RLKs, the involvement of the free hydroxyl group of gatekeeper Tyr in an H-bonding network cannot be considered as a quintessential signature of the activated state for all RLKs.

In an earlier report, we demonstrated SYMRK from *Arachis hypogaea* (*Ah*SYMRK) to predominantly autophosphorylate on gatekeeper Tyr (Y670) both in vitro and in planta (Samaddar et al., 2013). Apart from SYMRK, autophosphorylation of gatekeeper Tyr is only evidenced in BRI1 (Oh et al., 2009b). Autophosphorylation on gatekeeper Tyr was not a prerequisite for *Ah*SYMRK to be catalytically active, and hence the significance of gatekeeper phosphorylation remained elusive (Samaddar et al., 2013; Paul et al., 2014). Here we report the biochemical and biological importance of gatekeeper phosphorylation by demonstrating its role in autoactivation of *Ah*SYMRK and progress of RNS. *Ah*SYMRK with nonphosphorylatable residues in the gatekeeper position significantly increased or suppressed autophosphorylation on specific sites in the activation segment/αEF and β3-αC loop, indicating the identity of SYMRK's gatekeeper residue to be important for determining the state of autoactivation of this RLK. This change of autophosphorylation profile with nonphosphorylatable gatekeepers led to complete loss of coordination between rhizobial invasion in the epidermis and nodule organogenesis in the cortex in RNS restricting the rhizobia in the epidermal-cortical interface.

RESULTS

Gatekeeper Tyr Defines a Distinct Autoactivation State of *Ah*SYMRK

Gatekeeper Tyr (Y670) was identified previously as a potential site of autophosphorylation in *Ah*SYMRK by mutagenesis and sequence-specific antibodies both in vitro and in planta (Samaddar et al., 2013). Here we first verified Y670 phosphorylation by mass spectrometry to reconfirm phosphorylation on this residue (Fig. 1A; Supplemental Table S1). To probe into the importance of gatekeeper phosphorylation, we substituted Y670 with another hydroxyl-containing amino acid residue like Thr (Y670T), nonphosphorylatable residues like Phe or Ala (Y670F, Y670A), or a phosphomimic like Glu (Y670E) and monitored the catalytic consequences of the modifications in recombinant *Ah*SYMRK. The level of intrinsic autophosphorylation was higher in wild type and Y670T, but in vitro autophosphorylation activity was at least 4- to 5-fold higher in Y670F and Y670A (Fig. 1B). The phosphomimic substitution Y670E that permanently introduces a negative charge in the

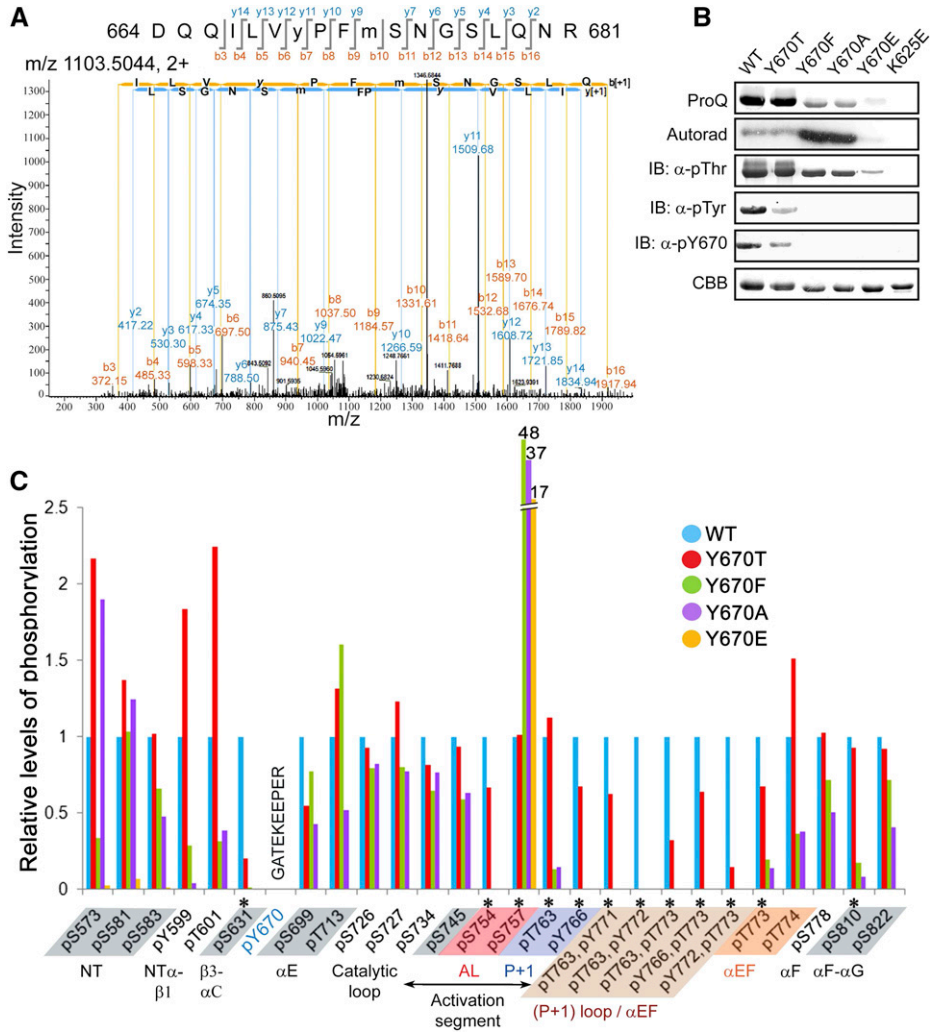

Figure 1. Gatekeeper Y670 defines a distinct autoactivation state for *Ah*SYMRK. A, *Ah*SYMRK is autophosphorylated on gatekeeper Y670. Product ion spectrum of a doubly charged peptide ion at *m/z* 1103.5044 with the phosphosite assigned to be Y670 in the sequence 664-DQQILVYPFMSNGSLQNR-681. B, Autophosphorylation of gatekeeper mutants. Intrinsic phosphorylation detected by ProQ Diamond staining, in vitro *Ah*SYMRK autophosphorylation activity detected by [^{32}P]γ-ATP (autorad), phosphorylation was detected by antiphosphothreonine (α-pThr), antiphosphotyrosine (α-pTyr), and modification specific (α-pY670: 665-674) antibodies, protein abundance visualized by Coomassie Brilliant Blue staining (CBB). The catalytically inactive K625E mutant is used as reference. C, Gatekeeper mutations significantly affect the autophosphorylation profile of *Ah*SYMRK. An MS-based quantitation of specific phosphopeptides from recombinant *Ah*SYMRK gatekeeper Y670 mutant proteins relative to WT (wild type, defined as 1). Phosphosites have been arranged N to C terminus and clustered under the typical secondary structural features of the kinase domain (Taylor and Kornev, 2011). Gatekeeper Y670/T670, S674, S677 (Supplemental Tables S2 and S3) have not been included due to different ionization efficiencies of these phosphopeptides. Phosphosites significantly affected due to Y670 substitutions have been marked with *. Activation loop (AL, red), P+1 loop (blue), αEF helix (orange), P+1 loop/ αEF (brown).

catalytic groove (Paul et al., 2014) drastically reduced both intrinsic and in vitro autophosphorylation activities of *Ah*SYMRK but did not render the kinase catalytically dead like K625E. While pThr was detectable in all the mutants, including Y670E, pTyr was only detectable in wild type and Y670T, indicating that a phosphorylatable residue in the gatekeeper position was necessary for the kinase to autophosphorylate on Tyr residues and become dual specific. Gatekeeper phosphorylation-specific antibody α-pY670 (665–674) recognized *Ah*SYMRK but did not react with its gatekeeper mutants like Y670F, Y670A, Y670E, or the catalytically dead mutant K625E, attesting to its specificity. But it was intriguing to note a feeble but consistent immunoblot cross-reactivity of α-pY670 (665–674) with Y670T, which we believe is due to phosphorylation on gatekeeper Thr (pT670) as suggested by MS analysis (Fig. 1B; Supplemental Table S2).

We then examined how the nature of the gatekeeper affected the relative levels of phosphorylation in each of the identified phosphorylation sites in *Ah*SYMRK using label-free quantitative mass spectrometry (Ahmed et al., 2014). Only phosphopeptides that were detected in all experimental replicates of the wild type and Y670T/F/A mutants were subjected to quantitation (Supplemental Tables S2 and S3). Additionally, we quantified Y670E phosphorylation status for these sites only, which was either absent or barely detectable. The pY-containing peptides encompassing the activation segment/αEF helix were only detectable in wild type and Y670T and have been included in the analysis. Representative data plotted against the functional domains of protein kinases highlighted the sharp contrast in the autophosphorylation profile between *Ah*SYMRK with phosphorylatable (Y670/Y670T) and nonphosphorylatable gatekeepers (Y670F/A; Fig. 1C). While autophosphorylation on most sites was relatively unaffected by gatekeeper substitution, in several sites autophosphorylation was selectively suppressed only in Y670F and Y670A. Those sites are located in the β3-αC loop (S631), activation segment (S754, T763), αEF helix (T773), and the αF-αG loop (S810). Besides, doubly phosphorylated peptides encompassing the P+1 loop and/or the αEF helix-containing pY766/pY771/pY772 were conspicuously absent in Y670F/A mutants, indicating this region to have a contrasting pY signature with nonphosphorylatable gatekeepers (Supplemental Table S3). As opposed to these sites, where autophosphorylation was compromised in Y670F/A, autophosphorylation in S757 residue in the activation loop showed a sharp increase in Y670F (approximately 48-fold) and Y670A (approximately 37-fold). Interestingly, Y670E polypeptide, which was barely active, showed an approximately 17-fold increase in autophosphorylation in S757 residue. Thus, two different autoactivation states with two distinct sets of autophosphorylation targets are defined in *Ah*SYMRK with phosphorylatable or nonphosphorylatable gatekeepers.

Nonphosphorylatable Gatekeepers in *Ah*SYMRK Arrested ITs in the Epidermis

Cross species complementation tests showed that SYMRKs from eurosids, including nodulating and nonnodulating lineages, can restore symbiosis in *symrk* null mutants (Gherbi et al., 2008; Markmann et al., 2008). Earlier we have demonstrated complementation of TR25, a *symrk* null mutant of *M. truncatula* by *Ah*SYMRK (Saha et al., 2014). The same experimental conditions were used to determine the significance of gatekeeper Y670 phosphorylation in *Ah*SYMRK in vivo, where we transformed TR25 with the native *Ah*SYMRK and its gatekeeper mutants and monitored their ability to restore symbiotic features. Transformed roots inoculated with *Sinorhizobium meliloti*-mRFP were monitored for their colonization at 2 weeks after infection (WAI). Upon infection with *S. meliloti*, in both TR25/*Ah*SYMRK and TR25/*Ah*SYMRK-Y670T roots, microcolonies were observed within tightly curled root hairs and IT formation could be restored (Fig. 2, A and B). In TR25/*Ah*SYMRK, the ITs were always a continuous tubular structure (Fig. 2A), whereas in TR25/*Ah*SYMRK-Y670T, ITs sometimes developed sac-like structures (Fig. 2C) or revealed misdirected progression at the epidermal-cortical interface (Fig. 2D), but in most cases the ITs were found to progress normally (Fig. 2E). In contrast, in TR25/*Ah*SYMRK-Y670F/A, the root hair curls were enlarged with diffused agglomerations (Fig. 2, F and J). In both cases the ITs contained extensive inflated sac-like structures, and this feature was more prominent in TR25/*Ah*SYMRK-Y670F roots (Fig. 2, F–H and J-L). However, the most important distinguishing feature was the arrest of IT progression at the epidermal cortical interface or subepidermal cortex (Fig. 2, F–H, J and L). The misdirected ITs were noted to migrate parallel to the longitudinal axis of the root instead of ramifying and reaching the dividing cortical cells (Fig. 2, H and I, L and M). ITs were also found to be blocked within the root hair shaft but that was rare (Fig. 2K). Also, as compared to TR25/*Ah*SYMRK and TR25/*Ah*SYMRK-Y670T/A, the number of ITs was at least approximately 3 times higher in only TR25/*Ah*SYMRK-Y670F (Fig. 2, N and O; Supplemental Fig. S1), which could be due to the plants' attempt to compensate for the defect in IT propagation (more prominent in Y670F) by initiation of more ITs, as noted before in *Lotus* (Murray et al., 2007). In contrast to these observations, none of the epidermal features of rhizobial invasion were restored in TR25/*Ah*SYMRK-Y670E roots, which is consistent with the drastic loss of catalytic activity in Y670E (Fig. 2P). In summary, with nonphosphorylatable gatekeepers in *Ah*SYMRK, the epidermal/cortical barrier was insurmountable by ITs. This is a direct demonstration of the physiological consequences of the differential autophosphorylation profile of *Ah*SYMRK with a phosphorylatable and a nonphosphorylatable gatekeeper.

Nonphosphorylatable Gatekeepers in *Ah*SYMRK Uncoupled Epidermal and Cortical Events in RNS

Our next objective was to monitor the gatekeeper substitution mutants of SYMRK for their ability to restore nodule organogenesis and rhizobial colonization in the cortex. By 6 WAI, nodules were visible with all the mutants, and their number was reproducibly higher (approximately 2–3 times) with all the gatekeeper substituted mutants (Supplemental Fig. S2; Supplemental Table S4). In TR25/*Ah*SYMRK and TR25/*Ah*SYMRK-Y670T, cortical ramification of ITs was restored, and the symbionts were released in the central infected zone of the developed nodule (n = 40; Fig. 3, A and B, J and K). However, some infected nodules in TR25/*Ah*SYMRK-Y670T were distinct by having a small infection patch/pocket at the apex, a feature almost never observed in nodules developed in TR25/*Ah*SYMRK roots (Fig. 3B). In at least 20% of TR25/*Ah*SYMRK-Y670T nodules, the misdirected ITs remained restricted in apical pockets, leaving the nodules without a central infected zone (Fig. 3A inset,

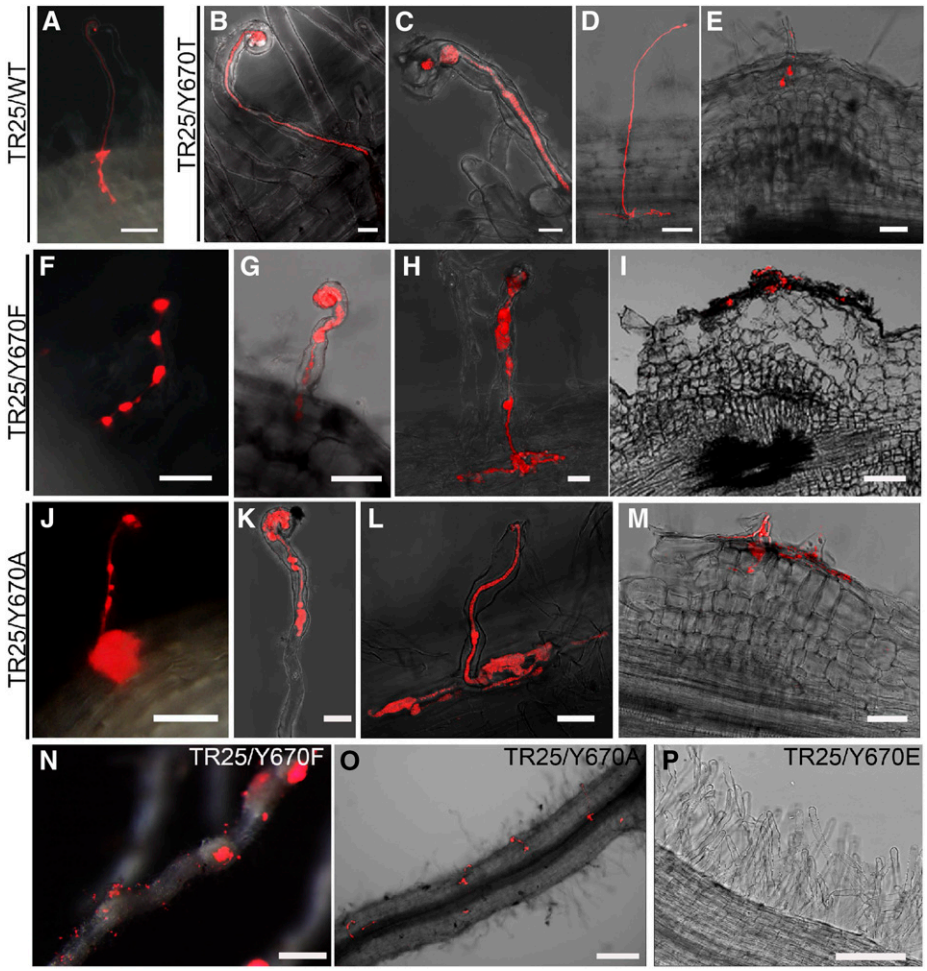

Figure 2. Effect of the gatekeeper mutation on progression of ITs. TR25 roots were transformed with *35S::AhSYMRK-GFP* and gatekeeper mutants *35S::AhSYMRK-Y670T/F/A/E-GFP*. Progress of IT was observed 2 WAI with *S. meliloti*-mRFP and is shown as merged images of bright field and mRFP fluorescence. IT progress in TR25/*Ah*SYMRK (A), TR25/*Ah*SYMRK-Y670T (B-E), TR25/ *Ah*SYMRK-Y670F (F-I), TR25/ *Ah*SYMRK-Y670A (J-M). No *S.meliloti* colonization was observed in roots of TR25/*Ah*SYMRK-Y670E (P). *S. meliloti* colonization in *Ah*SYMRK-Y670F (N) and *Ah*SYMRK-Y670A (O) roots. Scale bar: 200 μm (N-O), 100 μm (A, F, I-J, P), 50 μm (D-E, G, M), 20 μm (H, K-L) and 10 μm (B-C).

Figure 3, C and L). As opposed to TR25/*Ah*SYMRK-Y670T, in TR25/*Ah*SYMRK-Y670F/A nodules there was absolutely no ramification of ITs in the nodule interior (n = 60; Fig. 3, D-I, L). As a result, the nodules were always empty and the symbionts were strictly restricted to extensive infection patches on the apex. Moreover, the nodules developed in TR25/*Ah*SYMRK-Y670F/A showed improper vasculature (Fig. 3, E and H), which is in accordance with the adverse effect on nodule organogenesis by epidermal arrest of rhizobial invasion as demonstrated in both *Medicago* and *Lotus* (Yano et al., 2009; Guan et al., 2013). This effect was not ephemeral, as the symbionts were detained in the infection pockets without any signs of IT propagation to the cortex even 8 WAI, and the nodule development never progressed further. Additionally, TR25/*Ah*SYMRK-(573–883)-Y670F could profusely generate spontaneous nodules and these nodules developed with proper vasculature (Supplemental Fig. S3), as demonstrated earlier in TR25/*Ah*SYMRK-(573–883; Saha et al., 2014; Saha and DasGupta, 2015). This confirms that the restricted autoactivation of *Ah*SYMRK-Y670F can generate all the signals necessary for proper nodule organogenesis, and the improper vasculature noted in TR25/*Ah*SYMRK-Y670F/A was indeed due to inhibitory signals generated by epidermal arrest of symbionts. Also the increase of nodule number with gatekeeper mutants is likely to be a downstream effect of the absence of mature nodules, where absence of suppression may have led to a recurrent initiation of new foci of cell divisions as proposed previously in *Medicago* (Kuppusamy et al., 2004). These results again show a correlation between the RNS features and the differential autophosphorylation profile of SYMRK with a phosphorylatable and a nonphosphorylatable gatekeeper.

*Ah*SYMRK with Nonphosphorylatable Gatekeepers Fails to Up-Regulate Expression of Genes Required for Epidermal-Cortical Coordination in RNS

Several factors have been evidenced in the literature to have a role in epidermal-cortical coordination in RNS (Popp and Ott, 2011): for example, TFs like CYCLOPS (Singh et al., 2014) and NIN (Soyano et al., 2013; Vernié et al., 2015), a nodule-specific remorin *Mt*SYMREM1 (Lefebvre et al., 2010), the plasma membrane-resident ankyrin protein Vapyrin (Murray et al., 2011), the U-box containing E3 ubiquitin-ligase LIN (Kuppusamy et al., 2004), and the noncoding RNA ENOD40 (Crespi et al., 1994). In CYCLOPS mutant of *Medicago* (TE7), several nodules remain small (primordia), with ITs arrested at the nodule apex similar to what has been

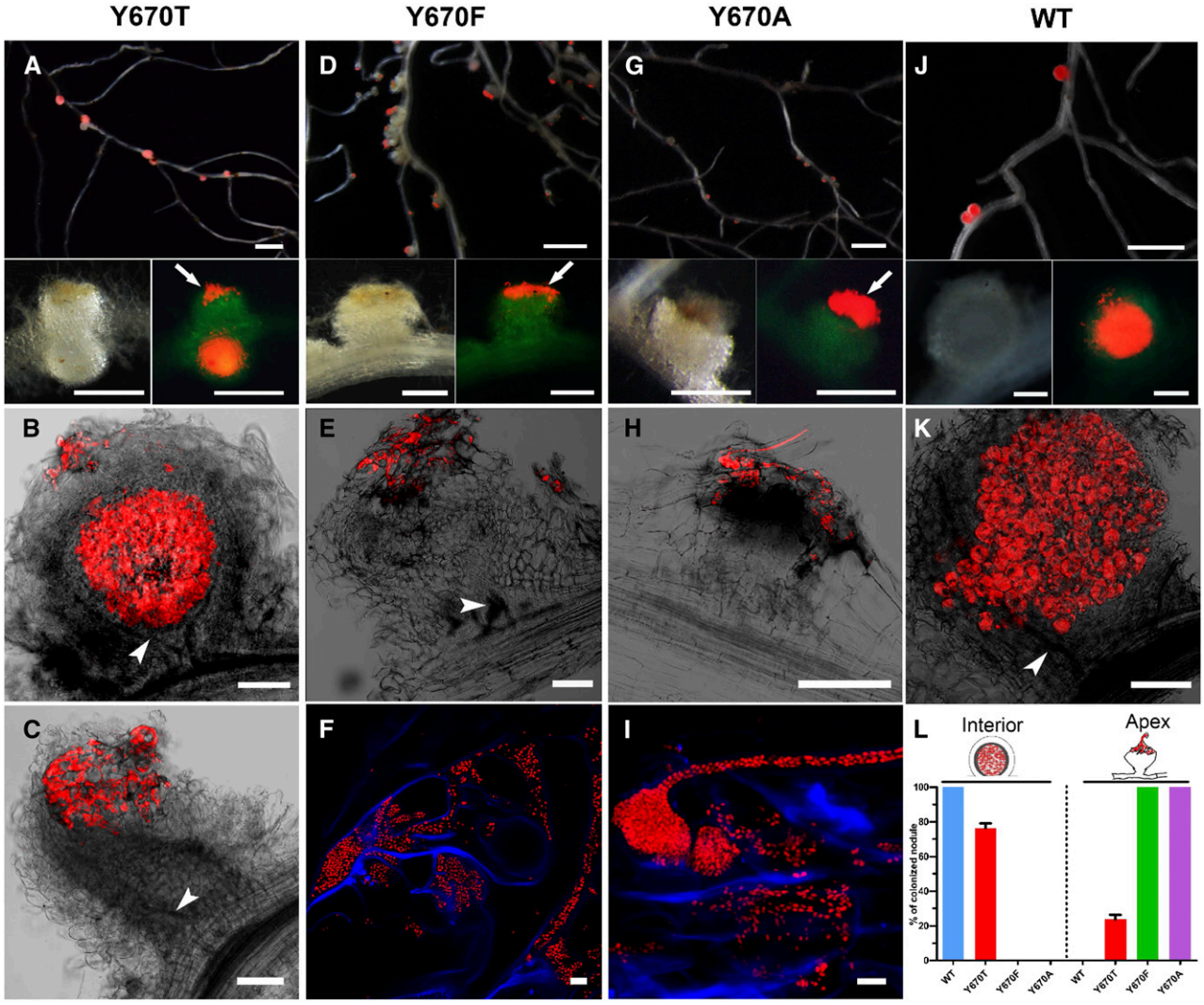

Figure 3. Effect of the gatekeeper mutation on nodule development and symbiont colonization. TR25 roots were transformed with *35S::AhSYMRK-GFP* and gatekeeper mutants *35S::AhSYMRK-Y670T/F/A-GFP*. Nodule development and *S. meliloti* colonization was observed 6 WAI. Nodule developed in TR25/*Ah*SYMRK-Y670T (A-C), TR25/ *Ah*SYMRK-Y670F (D-F), TR25/ *Ah*SYMRK-Y670A (G-I), and TR25/ *Ah*SYMRK (J-K). Nodulated roots (A, D, G, J) with insets showing enlarged view of nodules. Rhizobial accumulation at the nodule apex indicated by arrow. Longitudinal sections revealing *S. meliloti* colonized in nodule interior (B, K). Infection pocket (B) and extensive infection patches in nodule apex (C, E, H). Magnified view of infection pocket showing subepidermal rhizobial colonization (F and I). Vascular bundles indicated by arrowhead. (L) Percentage of *S. meliloti* colonization in the nodule interior or apex in TR25 plants transformed with indicated gatekeeper mutants. Images shown as merged images of bright-field and red (*S. meliloti* expressing mRFP) (A-C, D-E, G-H, J-K), bright-field (bottom left) and merged (bottom right) images of GFP and mRFP fluorescence (inset of A, D, G, J) or merged images of red and blue (Calcofluor, cell wall stain) fluorescence (F, I). Scale bar: 2 mm (A, D, G, J), 500 μm (inset of A, D, G, J), 100 μm (B-C, E, H, K), and 5 μm (F, I).

observed in presence of *Ah*SYMRK with the non-phosphorylatable gatekeepers (Fig. 3, D-I; Benaben et al., 1995). *Lj*CYCLOPS transactivates the *NIN* gene, a bifunctional membrane bound transcriptional coactivator (Singh et al., 2014). In both *Medicago* and *Lotus*, *NIN* is essential for IT initiation in the epidermis and nodule organogenesis in the cortex (Yoro et al., 2014; Fournier et al., 2015). *Mt*SYMREM1 interacts with SYMRK and NFRs to mediate their assembly in membrane rafts, and its down-regulation leads to IT arrest in epidermal cells (Lefebvre et al., 2010). Both *Vapyrin* and *LIN* mutants in *Medicago* show impaired growth of ITs that are blocked in the epidermis (Kuppusamy et al., 2004; Murray et al., 2011). Finally, *ENOD40*, an early Nod factor-induced gene, has a role in both infection and nodule primordia initiation as demonstrated in *Medicago* (Crespi et al., 1994). Overall, all these genes appear to have a role in proper invasion of ITs into the dividing cells of the nodule primordia in the cortex.

We compared the expression of these genes in TR25/ *Ah*SYMRK-Y670T/F/A/E roots at 6 WAI. In TR25/ *Ah*SYMRK-Y670E, expression of the above symbiotic

genes was barely detectable, which is in accordance with absence of any symbiotic response of these roots in presence of rhizobia (Fig. 4). Expression of *LIN* and *MtENOD40* was relatively unaffected in TR25/*Ah*SYMRK-Y670T/F/A, indicating their expression to be upstream or parallel to the pathway that leads to overcoming of the epidermal/cortical barrier. *Vapyrin* is the only factor that was almost equally affected in TR25/*Ah*SYMRK-Y670T/F/A. Therefore, Vapyrin does not appear to be connected with the sharp contrast between TR25/*Ah*SYMRK-Y670F/A and TR25/*Ah*SYMRK-Y670T with respect to loss of cortical colonization. On the other hand, misdirected IT progression in the epidermis is a common feature that distinguishes TR25/*Ah*SYMRK-Y670T/F/A from its wild-type counterpart, and this feature may be associated with low expression of *Vapyrin*. In TR25/*Ah*SYMRK-Y670F/A, expression was significantly lower for *MtNIN* (approximately 6–9 fold), *MtSYMREM1* (approximately 4-fold), and *IPD3* (approximately 2-fold) as compared to TR25/*Ah*SYMRK-Y670T, indicating these genes to be directly involved in synchronizing the epidermal and cortical events. This attests to the role of these factors in coupling the epidermal and cortical events as suggested previously and designates them to function downstream to SYMRK for the same.

DISCUSSION

Here, we demonstrate gatekeeper Tyr autophosphorylation as a hallmark of a distinct autoactivated state of *Ah*SYMRK that generates vital phospho-cues for progress in symbiosis. *Ah*SYMRK with nonphosphorylatable gatekeepers like Phe and Ala conspicuously up-regulate or suppress autophosphorylation in specific sites (Fig. 1C), notably in the activation segment/αEF and β3-αC loop, and in addition failed to support a coordinated epidermal and cortical response during establishment of RNS (Figs. 2 and 3).

The role of SYMRK in coordinating the epidermal and cortical responses was first noted in *symrk-3 snf-1* double mutants of *Lotus*, where ITs were occasionally noted to be misdirected and swollen and unable to reach the nodule primordia (Madsen et al., 2010). Another example is *symrk-14* in *Lotus* with a P386L substitution in the extracellular GDPC motif of SYMRK that prevents its ectodomain shedding (Kosuta et al., 2011; Antolín-Llovera et al., 2014a). Substitution in the GDPC motif does not affect IT formation or nodule organogenesis but restricts ITs to the epidermis. Our investigations reveal SYMRK with nonphosphorylatable gatekeepers to have a similar phenotypic output in *Medicago* (Figs. 2 and 3). Additionally, we show that the state of autoactivation differs with a nonphosphorylatable gatekeeper, where autophosphorylation on selective targets on activation segment/αEF and β3-αC loop are significantly affected or abolished (Fig. 1). The phenotypic overlap of *symrk14* mutant of *Lotus* and our observations on TR25/*Ah*SYMRK-Y670F/A in *Medicago* suggest SYMRK to have distinct autoactivation states based on the nature of its extracellular domains. SYMRK activity with its intact ectodomain triggers cortical cell division and the epidermal IT formation. Then ectodomain shedding switches SYMRK to another autoactivation state that enables gatekeeper phosphorylation and full-scale phosphorylation of activation segment/αEF and β3-αC loop of the receptor. Together, ectodomain shedding and gatekeeper phosphorylation could be a coupled switch that maintains a synchrony between epidermal and cortical events for precisely timing the crossing over of the epidermal-cortical barrier for endocytic accommodation of symbionts in the primordia. It remains to be seen whether and how the extracellular GDPC motif allosterically connects with the gatekeeper residue in the kinase domain to deliver the outputs required for a successful coordination of epidermal and cortical symbiotic features.

Several other mutants have indicated the epidermal-cortical interface to be an important checkpoint during the progress of RNS (Popp and Ott, 2011; Rival et al., 2012; Hayashi et al., 2014). Premature arrest of ITs in the epidermis and restriction of symbionts in infection patches in the nodule apex was observed in *ccamk-14* (Liao et al., 2012), *nap-1*, *pir-1*(Yokota et al., 2009), and *nena* (Groth et al., 2010) of *Lotus*. In *Medicago*, similar phenotypes were observed in *lyk3* (Smit et al., 2007), TE7 (Benaben et al., 1995), *api* (Teillet et al., 2008), and

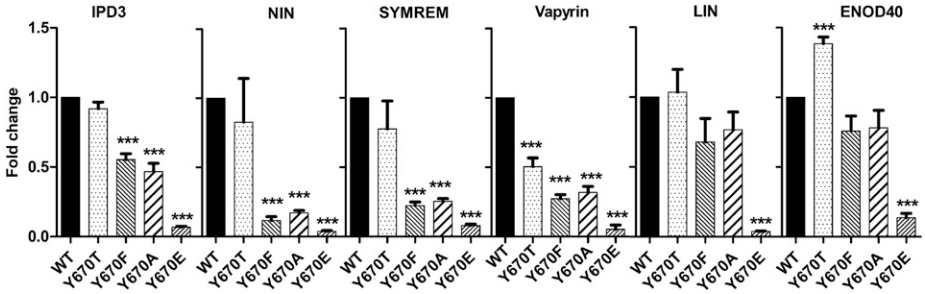

Figure 4. Effect of gatekeeper substitution on the expression of *IPD3*, *NIN*, *SYMREM1*, *Vapyrin*, *LIN*, and *ENOD40*. Expression of the mentioned genes in TR25/*Ah*SYMRK-Y670T/F/A/E at 6WAI was measured relative to those in TR25/*Ah*SYMRK roots. The expression level in TR25/*Ah*SYMRK was set to 1. In all cases, *Mt*ACTIN2 was used as the reference gene. Histograms represent means of three biological replicates ± SEM. Asterisks above bars indicate significant differences ($P < 0.05$).

lin-1 mutants (Kuppusamy et al., 2004). The spreading of misdirected ITs in the epidermis as noted predominantly with gatekeeper substituted SYMRKs in *Medicago* (TR25/*Ah*SYMRK-Y670F/A; Fig. 2) was previously noted in the *vag-1* and *suner1-1* mutants of *Lotus* (Suzaki et al., 2014; Yoon et al., 2014). The significance of CCaMK/DMI3 in epidermal-cortical crosstalk is illustrated in both *Lotus* and *Medicago* (Rival et al., 2012; Hayashi et al., 2014). Epidermal expression of CCaMK supported IT progression in the epidermis, but its cortical expression was essential for allowing the ITs to cross the epidermal/cortical barrier and triggering cortical cell division for nodule organogenesis. The Ca^{2+}-responsive domains of CCaMK were indispensable for epidermal infections but dispensable for nodule organogenesis and cortical infection processes (Gleason et al., 2006; Shimoda et al., 2012; Hayashi et al., 2014). NIN is also a central player in coordinating epidermal/cortical responses in both *Lotus* and *Medicago* (Soyano et al., 2013; Vernié et al., 2015). Overexpressing NIN in either the epidermis or the cortex auto-activates cortical cell division, but unlike epidermal NIN, cortical NIN expression can promote the formation of nodule like-structures independent of Cre1 (Vernié et al., 2015). Since SYMRK functions at the upstream end of the SYM pathway, the phenotypic overlap of TR25/*Ah*SYMRK-Y670F/A with the above mutants indicates SYMRK with its phospho-cues to be important for guiding the proper progression of the ITs. Additionally, expression of *MtNIN*, *MtSYMREM1*, and *IPD3* was significantly affected in TR25/*Ah*SYMRK-Y670F/A as compared to TR25/*Ah*SYMRK-Y670T (Fig. 4), indicating that these factors have important roles in enabling the ITs to surmount the epidermal-cortical barrier. All these genes are therefore involved in the network that guides and guards the epidermal-cortical barrier.

The sites where autophosphorylation was affected with a nonphosphorylatable gatekeeper (Y670F/A) are all conserved in SYMRKs from other species (Fig. 1C; Supplemental Fig. S4), indicating the strategic importance of gatekeeper phosphorylation and suggesting the underlying mechanism of full-scale autoactivation of SYMRKs to be conserved. Even in other RLKs, the same sites or regions are known to be autophosphorylated, suggesting the autoactivating principles to be conserved beyond SYMRK (Supplemental Fig. S4). The residue S757, where autophosphorylation sharply increased in absence of a phosphorylatable gatekeeper (Fig. 1C), is also highly conserved in SYMRKs, suggesting its importance in symbiotic signaling. Phosphorylation on the invariant Thr (T763 in *Ah*SYMRK/T760 in *Lj*SYMRK) in the activation loop was shown earlier to be important for SYMRK activity (Yoshida and Parniske, 2005; Samaddar et al., 2013). Since T763 autophosphorylation is drastically down-regulated in Y670F/A, it could be that the autoactivation with a nonphosphorylatable gatekeeper is actually independent of T763 phosphorylation in the activation segment. Such activation loop phosphorylation-independent activation is demonstrated in certain RTKs and RLKs (Dardick et al., 2012; Plaza-Menacho et al., 2014).

It remains to be understood as to how gatekeeper Tyr phosphorylation in the hinge region is involved with autophosphorylation in the distal and dynamic elements like the activation segment/αEF helix and β3-αC loop (Fig. 1C). However, the importance of hinge motions for kinase activation and allosteric communication between the activation loop and hinge has been suggested for some animal kinases (Hari et al., 2013; Sours et al., 2014). In the majority of RTKs, an inhibitory network of hydrogen bonds involving the gatekeeper residue is disengaged upon activation loop phosphorylation to activate the kinase (Chen et al., 2007). In ERK2, flexibility of the activation loop and its accessibility to autophosphorylation could be controlled over long distances by the nature of the gatekeeper through an intramolecular pathway of connectivity through interacting side chains (Emrick et al., 2006). A similar mechanism has been hypothesized for Arabidopsis (*Arabidopsis thaliana*) MPK6, where gatekeeper Tyr substitutions lead to constitutive activity and independence from upstream MAPK activation (Berriri et al., 2012). In tune with these examples, our results indicate SYMRK adopts such long-range allosteric interaction networks whereby it transmits the identity of the gatekeeper to distant locations within the core kinase domain for full-scale autoactivation of the kinase. Consistent with this proposition, we have already demonstrated that conformations of SYMRK distinctly differ based on whether it had Tyr or Phe as the gatekeeper (Paul et al., 2014). We hypothesize the phosphorylated or nonphosphorylated state of the gatekeeper Tyr to determine the autophosphorylation trajectory in SYMRK as described for the FGFR family of animal kinases and thereby define distinct autoactivation states (Furdui et al., 2006). Further experimentation is required for determining the state of phosphorylation of SYMRK with the initiation and progress of symbiosis to understand how well the in vitro phosphorylation studies reflect the trajectory of its autophosphorylation in planta. Such understanding would clarify the role of differential phosphoclusters of SYMRK in serving as a platform for 'docking' of effector proteins to transmit downstream signaling.

In conclusion, a phosphorylatable gatekeeper residue determines a distinct autoactivation state of SYMRK that differentially autophosphorylates and generates phospho-cues for coupling the epidermal and cortical responses of RNS. Since a gatekeeper Tyr is common in RLKs, a conserved mechanism of activation associated with gatekeeper phosphorylation could be of common occurrence in RLKs.

MATERIALS AND METHODS

Plant and Rhizobial Strains

Medicago TR25 seeds, *Agrobacterium rhizogenes* strain MSU440, and *pBHR-mRFP-Sinorhizobium meliloti* 2011 strain were used.

Constructs

pET28a-AhSYMRK-kd(573-883)(Samaddar et al., 2013) and its point mutations generated with the QuikChangeSite-Directed mutagenesis kit (Stratagene) were

used to express the His_6-polypeptides in *Escherichia coli* strain BL21 (DE3). The full-length *AhSYMRK* and its gatekeeper mutants *AhSYMRK-Y670T/F/A/E* were recombined into pK7FWG2 using LR-Clonase (Life Technologies), thereby generating *35S::AhSYMRK-GFP* and its corresponding Tyr residue mutants, for example *35S::AhSYMRK-Y670T/F/A/E-GFP* (for details, see Supplemental Methods S1).

Kinase Assay, Phosphoamino Acid Analysis, and Immunoprecipitation

Kinase autophosphorylation assays, immunoblotting, immunoprecipitation and phosphostaining were performed as described previously (DasGupta, 1994; Samaddar et al., 2013; Paul et al., 2014).

Label-Free Quantitative Mass Spectrometry

The recombinant proteins were subjected to the kinase reaction with unlabeled ATP until phosphorylation was complete, followed by sample preparation and LC-MS/MS analysis as described in Supplemental Methods S1.

Phenotypic Analysis

Generation of composite *Medicago truncatula* plants and scoring nodulation, phenotypic analysis, and confocal microscopy were performed as described previously (Saha et al., 2014).

For detailed description of methods pertaining to construct generation, quantitative RT-PCR, primers used, see Supplemental Methods S1.

Supplemental Data

The following supplemental materials are available.

Supplemental Figure S1. ITs in TR25/*Ah*SYMRK and TR25/*Ah*SYMRK-Y670T/F/A roots 2 WAI with *S. meliloti*.

Supplemental Figure S2. Nodules developed in TR25/*Ah*SYMRK and TR25/*Ah*SYMRK-Y670T/F/A roots 6 WAI with *S. meliloti*.

Supplemental Figure S3. Spontaneous nodule formation by overexpression of *Ah*SYMRK-(573–883) Y670F.

Supplemental Figure S4. Conservation of phosphorylation sites in SYMRKs and other RLKs.

Supplemental Table S1. Phosphorylation on gatekeeper Y670 of wild-type *Ah*SYMRK-kd identified by LC-MS/MS.

Supplemental Table S2. List of phosphorylation sites detected for *Ah*SYMRK-kd and its gatekeeper mutants, identified by LC-MS/MS.

Supplemental Table S3. List of phosphopeptides of *Ah*SYMRK-kd and its gatekeeper mutants quantitated by LFQMS (represented in Fig. 1C).

Supplemental Table S4. Restoration of RNS in TR25 by overexpression of *AhSYMRK* and *AhSYMRK-Y670T/F/A/E*.

Supplemental Methods S1. Methods in detail.

ACKNOWLEDGMENTS

We thank Giles Oldroyd and Christian Rogers for TR25 seeds, Ton Bisseling and Erik Limpens for *S. meliloti* harboring *pBHR-mRFP*, and Douglas R. Cook for *Agrobacterium* strain MSU440.

Received December 18, 2015; accepted March 9, 2016; published March 9, 2016.

LITERATURE CITED

Ahmed S, Grant KG, Edwards LE, Rahman A, Cirit M, Goshe MB, Haugh JM (2014) Data-driven modeling reconciles kinetics of ERK phosphorylation, localization, and activity states. Mol Syst Biol **10:** 718

Antolín-Llovera M, Petutsching EK, Ried MK, Lipka V, Nürnberger T, Robatzek S, Parniske M (2014b) Knowing your friends and foes–plant receptor-like kinases as initiators of symbiosis or defence. New Phytol **204:** 791–802

Antolín-Llovera M, Ried MK, Parniske M (2014a) Cleavage of the SYMBIOSIS RECEPTOR-LIKE KINASE ectodomain promotes complex formation with Nod factor receptor 5. Curr Biol **24:** 422–427

Azam M, Seeliger MA, Gray NS, Kuriyan J, Daley GQ (2008) Activation of tyrosine kinases by mutation of the gatekeeper threonine. Nat Struct Mol Biol **15:** 1109–1118

Benaben V, Duc G, Lefebvre V, Huguet T (1995) TE7, An Inefficient Symbiotic Mutant of Medicago truncatula Gaertn. cv Jemalong. Plant Physiol **107:** 53–62

Berriri S, Garcia AV, Frei dit Frey N, Rozhon W, Pateyron S, Leonhardt N, Montillet JL, Leung J, Hirt H, Colcombet J (2012) Constitutively active mitogen-activated protein kinase versions reveal functions of Arabidopsis MPK4 in pathogen defense signaling. Plant Cell **24:** 4281–4293

Bojar D, Martinez J, Santiago J, Rybin V, Bayliss R, Hothorn M (2014) Crystal structures of the phosphorylated BRI1 kinase domain and implications for brassinosteroid signal initiation. Plant J **78:** 31–43

Broghammer A, Krusell L, Blaise M, Sauer J, Sullivan JT, Maolanon N, Vinther M, Lorentzen A, Madsen EB, Jensen KJ, et al (2012) Legume receptors perceive the rhizobial lipochitin oligosaccharide signal molecules by direct binding. Proc Natl Acad Sci USA **109:** 13859–13864

Chen H, Ma J, Li W, Eliseenkova AV, Xu C, Neubert TA, Miller WT, Mohammadi M (2007) A molecular brake in the kinase hinge region regulates the activity of receptor tyrosine kinases. Mol Cell **27:** 717–730

Crespi MD, Jurkevitch E, Poiret M, d'Aubenton-Carafa Y, Petrovics G, Kondorosi E, Kondorosi A (1994) enod40, a gene expressed during nodule organogenesis, codes for a non-translatable RNA involved in plant growth. EMBO J **13:** 5099–5112

Dardick C, Schwessinger B, Ronald P (2012) Non-arginine-aspartate (non-RD) kinases are associated with innate immune receptors that recognize conserved microbial signatures. Curr Opin Plant Biol **15:** 358–366

DasGupta M (1994) Characterization of a calcium-dependent protein kinase from Arachis hypogea (groundnut) seeds. Plant Physiol **104:** 961–969

Emrick MA, Lee T, Starkey PJ, Mumby MC, Resing KA, Ahn NG (2006) The gatekeeper residue controls autoactivation of ERK2 via a pathway of intramolecular connectivity. Proc Natl Acad Sci USA **103:** 18101–18106

Endre G, Kereszt A, Kevei Z, Mihacea S, Kaló P, Kiss GB (2002) A receptor kinase gene regulating symbiotic nodule development. Nature **417:** 962–966

Fournier J, Teillet A, Chabaud M, Ivanov S, Genre A, Limpens E, de Carvalho-Niebel F, Barker DG (2015) Remodeling of the infection chamber before infection thread formation reveals a two-step mechanism for rhizobial entry into the host legume root hair. Plant Physiol **167:** 1233–1242

Furdui CM, Lew ED, Schlessinger J, Anderson KS (2006) Autophosphorylation of FGFR1 kinase is mediated by a sequential and precisely ordered reaction. Mol Cell **21:** 711–717

Gage DJ (2004) Infection and invasion of roots by symbiotic, nitrogen-fixing rhizobia during nodulation of temperate legumes. Microbiol Mol Biol Rev **68:** 280–300

Gherbi H, Markmann K, Svistoonoff S, Estevan J, Autran D, Giczey G, Auguy F, Péret B, Laplaze L, Franche C, et al (2008) SymRK defines a common genetic basis for plant root endosymbioses with arbuscular mycorrhiza fungi, rhizobia, and Frankiabacteria. Proc Natl Acad Sci USA **105:** 4928–4932

Gleason C, Chaudhuri S, Yang T, Muñoz A, Poovaiah BW, Oldroyd GE (2006) Nodulation independent of rhizobia induced by a calcium-activated kinase lacking autoinhibition. Nature **441:** 1149–1152

Groth M, Takeda N, Perry J, Uchida H, Dräxl S, Brachmann A, Sato S, Tabata S, Kawaguchi M, Wang TL, et al (2010) NENA, a Lotus japonicus homolog of Sec13, is required for rhizodermal infection by arbuscular mycorrhiza fungi and rhizobia but dispensable for cortical endosymbiotic development. Plant Cell **22:** 2509–2526

Guan D, Stacey N, Liu C, Wen J, Mysore KS, Torres-Jerez I, Vernié T, Tadege M, Zhou C, Wang ZY, et al (2013) Rhizobial infection is associated with the development of peripheral vasculature in nodules of Medicago truncatula. Plant Physiol **162:** 107–115

Hari SB, Merritt EA, Maly DJ (2013) Sequence determinants of a specific inactive protein kinase conformation. Chem Biol **20:** 806–815

Hayashi T, Shimoda Y, Sato S, Tabata S, Imaizumi-Anraku H, Hayashi M (2014) Rhizobial infection does not require cortical expression of

upstream common symbiosis genes responsible for the induction of Ca(2+) spiking. Plant J **77:** 146–159

Kawaharada Y, Kelly S, Nielsen MW, Hjuler CT, Gysel K, Muszyński A, Carlson RW, Thygesen MB, Sandal N, Asmussen MH, et al (2015) Receptor-mediated exopolysaccharide perception controls bacterial infection. Nature **523:** 308–312

Klaus-Heisen D, Nurisso A, Pietraszewska-Bogiel A, Mbengue M, Camut S, Timmers T, Pichereaux C, Rossignol M, Gadella TW, Imberty A, et al (2011) Structure-function similarities between a plant receptor-like kinase and the human interleukin-1 receptor-associated kinase-4. J Biol Chem **286:** 11202–11210

Kosuta S, Held M, Hossain MS, Morieri G, Macgillivary A, Johansen C, Antolín-Llovera M, Parniske M, Oldroyd GE, Downie AJ, et al (2011) Lotus japonicus symRK-14 uncouples the cortical and epidermal symbiotic program. Plant J **67:** 929–940

Kuppusamy KT, Endre G, Prabhu R, Penmetsa RV, Veereshlingam H, Cook DR, Dickstein R, Vandenbosch KA (2004) LIN, a Medicago truncatula gene required for nodule differentiation and persistence of rhizobial infections. Plant Physiol **136:** 3682–3691

Lefebvre B, Timmers T, Mbengue M, Moreau S, Hervé C, Tóth K, Bittencourt-Silvestre J, Klaus D, Deslandes L, Godiard L, et al (2010) A remorin protein interacts with symbiotic receptors and regulates bacterial infection. Proc Natl Acad Sci USA **107:** 2343–2348

Lévy J, Bres C, Geurts R, Chalhoub B, Kulikova O, Duc G, Journet EP, Ané JM, Lauber E, Bisseling T, et al (2004) A putative Ca2+ and calmodulin-dependent protein kinase required for bacterial and fungal symbioses. Science **303:** 1361–1364

Liao J, Singh S, Hossain MS, Andersen SU, Ross L, Bonetta D, Zhou Y, Sato S, Tabata S, Stougaard J, et al (2012) Negative regulation of CCaMK is essential for symbiotic infection. Plant J **72:** 572–584

Limpens E, Franken C, Smit P, Willemse J, Bisseling T, Geurts R (2003) LysM domain receptor kinases regulating rhizobial Nod factor-induced infection. Science **302:** 630–633

Lin W, Li B, Lu D, Chen S, Zhu N, He P, Shan L (2014) Tyrosine phosphorylation of protein kinase complex BAK1/BIK1 mediates Arabidopsis innate immunity. Proc Natl Acad Sci USA **111:** 3632–3637

Madsen EB, Madsen LH, Radutoiu S, Olbryt M, Rakwalska M, Szczyglowski K, Sato S, Kaneko T, Tabata S, Sandal N, et al (2003) A receptor kinase gene of the LysM type is involved in legume perception of rhizobial signals. Nature **425:** 637–640

Madsen LH, Tirichine L, Jurkiewicz A, Sullivan JT, Heckmann AB, Bek AS, Ronson CW, James EK, Stougaard J (2010) The molecular network governing nodule organogenesis and infection in the model legume Lotus japonicus. Nat Commun **1:** 10

Markmann K, Giczey G, Parniske M (2008) Functional adaptation of a plant receptor-kinase paved the way for the evolution of intracellular root symbioses with bacteria. PLoS Biol **6:** e68

Messinese E, Mun JH, Yeun LH, Jayaraman D, Rougé P, Barre A, Lougnon G, Schornack S, Bono JJ, Cook DR, Ané JM (2007) A novel nuclear protein interacts with the symbiotic DMI3 calcium- and calmodulin-dependent protein kinase of Medicago truncatula. Mol Plant Microbe Interact **20:** 912–921

Miri M, Janakirama P, Held M, Ross L, Szczyglowski K (2016) Into the root: how cytokinin controls rhizobial infection. Trends Plant Sci**21:** 178–186

Mitra RM, Gleason CA, Edwards A, Hadfield J, Downie JA, Oldroyd GE, Long SR (2004) A Ca2+/calmodulin-dependent protein kinase required for symbiotic nodule development: gene identification by transcript-based cloning. Proc Natl Acad Sci USA **101:** 4701–4705

Miwa H, Sun J, Oldroyd GE, Downie JA (2006) Analysis of Nod-factor-induced calcium signaling in root hairs of symbiotically defective mutants of Lotus japonicus. Mol Plant Microbe Interact **19:** 914–923

Murray JD, Karas BJ, Sato S, Tabata S, Amyot L, Szczyglowski K (2007) A cytokinin perception mutant colonized by Rhizobium in the absence of nodule organogenesis. Science **315:** 101–104

Murray JD, Muni RR, Torres-Jerez I, Tang Y, Allen S, Andriankaja M, Li G, Laxmi A, Cheng X, Wen J, et al (2011) Vapyrin, a gene essential for intracellular progression of arbuscular mycorrhizal symbiosis, is also essential for infection by rhizobia in the nodule symbiosis of Medicago truncatula. Plant J **65:** 244–252

Oh M-H, Clouse SD, Huber SC (2009a) Tyrosine phosphorylation in brassinosteroid signaling. Plant Signal Behav **4:** 1182–1185

Oh MH, Wang X, Kota U, Goshe MB, Clouse SD, Huber SC (2009b) Tyrosine phosphorylation of the BRI1 receptor kinase emerges as a component of brassinosteroid signaling in Arabidopsis. Proc Natl Acad Sci USA **106:** 658–663

Oldroyd GE (2013) Speak, friend, and enter: signalling systems that promote beneficial symbiotic associations in plants. Nat Rev Microbiol **11:** 252–263

Paul A, Samaddar S, Bhattacharya A, Banerjee A, Das A, Chakrabarti S, DasGupta M (2014) Gatekeeper tyrosine phosphorylation is autoinhibitory for Symbiosis Receptor Kinase. FEBS Lett **588:** 2881–2889

Plaza-Menacho I, Barnouin K, Goodman K, Martínez-Torres RJ, Borg A, Murray-Rust J, Mouilleron S, Knowles P, McDonald NQ (2014) Oncogenic RET kinase domain mutations perturb the autophosphorylation trajectory by enhancing substrate presentation in trans. Mol Cell **53:** 738–751

Popp C, Ott T (2011) Regulation of signal transduction and bacterial infection during root nodule symbiosis. Curr Opin Plant Biol **14:** 458–467

Rival P, de Billy F, Bono JJ, Gough C, Rosenberg C, Bensmihen S (2012) Epidermal and cortical roles of NFP and DMI3 in coordinating early steps of nodulation in Medicago truncatula. Development **139:** 3383–3391

Saha S, DasGupta M (2015) Does SUNN-SYMRK crosstalk occur in Medicago truncatula for regulating nodule organogenesis? Plant Signal Behav **10:** e1028703

Saha S, Dutta A, Bhattacharya A, DasGupta M (2014) Intracellular catalytic domain of symbiosis receptor kinase hyperactivates spontaneous nodulation in absence of rhizobia. Plant Physiol **166:** 1699–1708

Samaddar S, Dutta A, Sinharoy S, Paul A, Bhattacharya A, Saha S, Chien KY, Goshe MB, DasGupta M (2013) Autophosphorylation of gatekeeper tyrosine by symbiosis receptor kinase. FEBS Lett **587:** 2972–2979

Shimoda Y, Han L, Yamazaki T, Suzuki R, Hayashi M, Imaizumi-Anraku H (2012) Rhizobial and fungal symbioses show different requirements for calmodulin binding to calcium calmodulin-dependent protein kinase in Lotus japonicus. Plant Cell **24:** 304–321

Shiu S-H, Bleecker AB (2001) Receptor-like kinases from Arabidopsis form a monophyletic gene family related to animal receptor kinases. Proc Natl Acad Sci USA **98:** 10763–10768

Singh S, Katzer K, Lambert J, Cerri M, Parniske M (2014) CYCLOPS, a DNA-binding transcriptional activator, orchestrates symbiotic root nodule development. Cell Host Microbe **15:** 139–152

Smit P, Limpens E, Geurts R, Fedorova E, Dolgikh E, Gough C, Bisseling T (2007) Medicago LYK3, an entry receptor in rhizobial nodulation factor signaling. Plant Physiol **145:** 183–191

Sohl CD, Ryan MR, Luo B, Frey KM, Anderson KS (2015) Illuminating the molecular mechanisms of tyrosine kinase inhibitor resistance for the FGFR1 gatekeeper mutation: the Achilles' heel of targeted therapy. ACS Chem Biol **10:** 1319–1329

Sours KM, Xiao Y, Ahn NG (2014) Extracellular-regulated kinase 2 is activated by the enhancement of hinge flexibility. J Mol Biol **426:** 1925–1935

Soyano T, Kouchi H, Hirota A, Hayashi M (2013) Nodule inception directly targets NF-Y subunit genes to regulate essential processes of root nodule development in Lotus japonicus. PLoS Genet **9:** e1003352

Stracke S, Kistner C, Yoshida S, Mulder L, Sato S, Kaneko T, Tabata S, Sandal N, Stougaard J, Szczyglowski K, et al (2002) A plant receptor-like kinase required for both bacterial and fungal symbiosis. Nature **417:** 959–962

Suzaki T, Ito M, Yoro E, Sato S, Hirakawa H, Takeda N, Kawaguchi M (2014) Endoreduplication-mediated initiation of symbiotic organ development in Lotus japonicus. Development **141:** 2441–2445

Suzaki T, Yoro E, Kawaguchi M (2015) Leguminous plants: inventors of root nodules to accommodate symbiotic bacteria. Int Rev Cell Mol Biol **316:** 111–158

Taylor SS, Kornev AP (2011) Protein kinases: evolution of dynamic regulatory proteins. Trends Biochem Sci **36:** 65–77

Teillet A, Garcia J, de Billy F, Gherardi M, Huguet T, Barker DG, de Carvalho-Niebel F, Journet EP (2008) api, A novel Medicago truncatula symbiotic mutant impaired in nodule primordium invasion. Mol Plant Microbe Interact **21:** 535–546

Vernié T, Kim J, Frances L, Ding Y, Sun J, Guan D, Niebel A, Gifford ML, de Carvalho-Niebel F, Oldroyd GE (2015) The NIN transcription factor coordinates diverse nodulation programs in different tissues of the Medicago truncatula root. Plant Cell **27:** 3410–3424

Yano K, Shibata S, Chen WL, Sato S, Kaneko T, Jurkiewicz A, Sandal N, Banba M, Imaizumi-Anraku H, Kojima T, et al (2009) CERBERUS, a novel U-box protein containing WD-40 repeats, is required for formation

of the infection thread and nodule development in the legume-Rhizobium symbiosis. Plant J **60:** 168–180

Yokota K, Fukai E, Madsen LH, Jurkiewicz A, Rueda P, Radutoiu S, Held M, Hossain MS, Szczyglowski K, Morieri G, et al (2009) Rearrangement of actin cytoskeleton mediates invasion of Lotus japonicus roots by Mesorhizobium loti. Plant Cell **21:** 267–284

Yoon HJ, Hossain MS, Held M, Hou H, Kehl M, Tromas A, Sato S, Tabata S, Andersen SU, Stougaard J, et al (2014) Lotus japonicus SUNERGOS1 encodes a predicted subunit A of a DNA topoisomerase VI that is required for nodule differentiation and accommodation of rhizobial infection. Plant J **78:** 811–821

Yoro E, Suzaki T, Toyokura K, Miyazawa H, Fukaki H, Kawaguchi M (2014) A positive regulator of nodule organogenesis, NODULE INCEPTION, acts as a negative regulator of rhizobial infection in Lotus japonicus. Plant Physiol **165:** 747–758

Yoshida S, Parniske M (2005) Regulation of plant symbiosis receptor kinase through serine and threonine phosphorylation. J Biol Chem **280:** 9203–9209